De-ghosting by kurtosis maximisation in practice

Sergio Grion, Rob Telling and Janet Barnes, Dolphin Geophysical*

Summary

Adaptive de-ghosting estimates the parameters of the physical process determining the ghost reflection, which are not generally precisely known. By application of incorrect de-ghosting parameters, the ghost is only partially removed and a residual ghost energy train manifests as a sequence of peaks and troughs with periodicity and amplitudes determined by the de-ghosting parameters. This residual ghost energy is often referred to as “ringing”, in data processing practice. The kurtosis of the de-ghosted data autocorrelation is strongly sensitive to the presence of this residual ghost energy. In this paper, we discuss the practice of adaptive de-ghosting by kurtosis maximization (Grion et al., 2015). We highlight the main features of the proposed algorithm using a simple synthetic example, and then present and discuss a field data application result.

Introduction

The sea-surface reflection coefficient can be frequency-dependent (see for example Clay and Medwin, 1977; Orji et al., 2013) and it is in general not a-priori known, the exception being the case of a perfectly calm sea-surface. Also, the receiver depth is subject to positioning inaccuracies, and the receiver depth measured during acquisition is subject to spatial interpolation and time averaging. Additionally, the shallow water column between the receiver and the sea surface is where the water velocity is most subject to variability, being closest to the surface and its associated temperature and salinity changes due to weather and tides. Sea surface reflectivity, water velocity and receiver depth are known with a good degree of approximation that is sufficient for a variety of processing steps, like multiple attenuation and migration, but de-ghosting is highly sensitive to these parameters. This is due to the combination of two factors: the strong amplitude and phase changes that ghost interference imposes on seismic data, and the fact that in the frequency domain these changes are at their strongest in correspondence with the ghost notches, where the signal to noise ratio of the recorded data is at its minimum. There is therefore a general need to estimate a physical model for the ghost reflection as part of a de-ghosting process.

Wang et al. (2013) discuss a bootstrap de-ghosting approach that requires the joint use of pre-migration data and its mirror, and optimizes the time-delay between primary and ghost. The authors do not attempt the estimation of the reflection coefficient. Masoomzadeh et al. (2013) point out that de-ghosting errors can be reduced by using a stochastic search for the optimum set of de-ghosting parameters that includes both delay-times and reflection coefficients that can vary with frequency. However, the search criteria or, in other words the objective function for optimisation of parameters, is not mentioned. Grion et al. (2013) compare de-ghosting results in the presence of calm and rough seas, and note that an adaptive de-ghosting that includes a statistical element is able to compensate rough sea effects for structural imaging purposes.

Adaptive de-ghosting by kurtosis maximization

In adaptive de-ghosting, it is important to stress that the aim is the estimation of "effective" parameters that best fulfil the objective of removing ghost reflections. These effective parameters are certainly linked to the physical properties of the water column above the streamer array, but they are also a function of ghost modelling assumptions, for example:

- Constant water velocity.
- Specular reflection at the sea surface (scattering is ignored).
- 2D wave-field propagation.
- Known receiver locations.

The physical entities determining the receiver ghost are the sea surface, the receiver depth and the water velocity and for de-ghosting purposes they can be represented by an effective ghost delay-time and sea surface reflection coefficient. The ghost model is:

$$G = 1 + r(f)e^{-j\omega g_t},$$

where $r(f)$ is the frequency-dependent reflection coefficient, ω is the angular frequency and g_t is the delay time between primary and ghost. This model is defined in the τ-p domain to accommodate 2D wavefield propagation, and g_t is therefore a function of the cable depth profile, water velocity and of the propagation angle. For the purpose of de-ghosting optimisation, $r(f)$ is assumed to be close to 1 at ω=0 and for higher frequencies it can either follow an a-priori parametric function (see e.g. Clay and Medwin, 1977) or it can be estimated at a limited number of frequencies, typically the notch frequencies, and then interpolated.

The optimisation metric we employ is based on the kurtosis of the de-ghosted-data autocorrelation. The kurtosis is a statistical measure often used to associate a measure of "peakedness" to a random variable x with mean η, expected

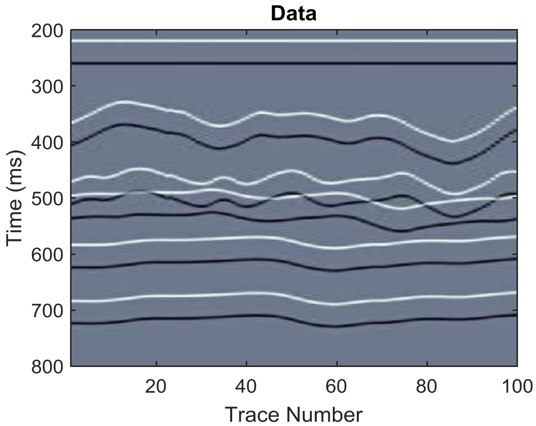

Figure 1: Synthetic data representative of a common-*p* section, where the delay time between ghost and primary is constant. Primary events appear as white pulses, and the associated black ghosts have a 40msec delay with respect to the primaries.

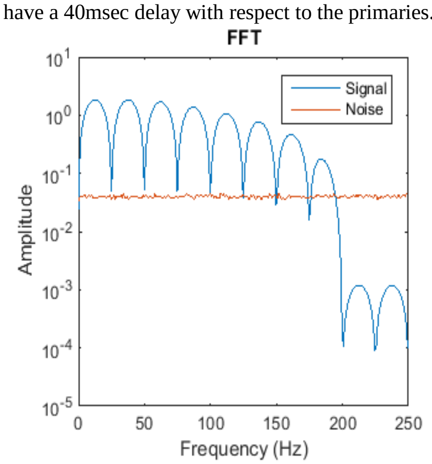

Figure 2: Amplitude spectra of signal and noise levels in Figure 1

to be non-Gaussian, and it is defined as:

$$k = \frac{\mu_4}{\sigma^4}, \qquad (1)$$

where $\mu_4 = E[(x-\eta)^4]$ is the 4th order central moment of x, and σ its standard deviation. Various authors have considered the kurtosis for wavelet estimation purposes (e.g. Cambois and Hargreaves, 1994; Van der Baan, 2008).

To illustrate the use of the proposed kurtosis-based metric to assess de-ghosting quality, we consider the following example. Figure 1 shows a synthetic dataset consisting of a sequence of primaries and ghosts. The delay of the ghosts with respect to primaries is 40ms, as expected from a 30m cable depth, and the reflection coefficient is -0.95. The data is contaminated by Gaussian white noise, and the amplitude spectra of signal and noise are shown in Figure 2. The

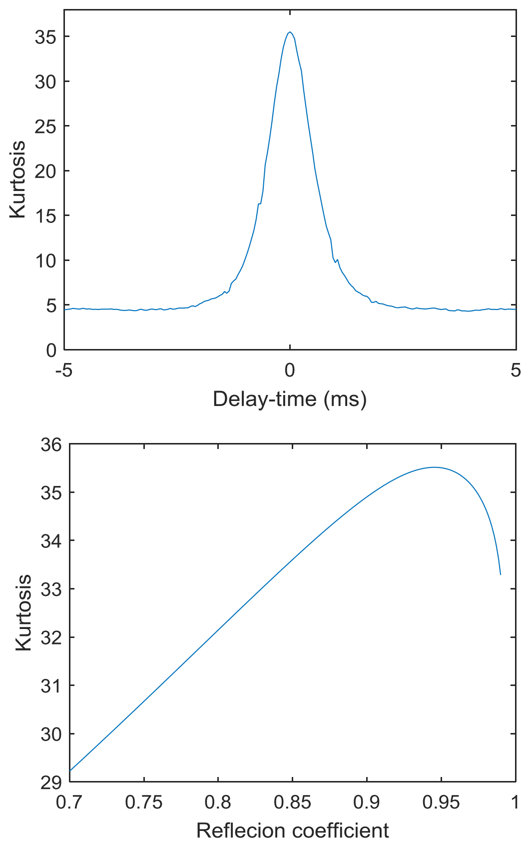

Figure 3: Kurtosis of delay-time estimation (top) and reflection coefficient estimation (bottom)

signal to noise ratio is variable with frequency, and has maximum values in the range 10-30dB in correspondence to the constructive interference between primary and ghost, and minimum values in the range 2dB to -7dB in correspondence with the ghost notches. The presence of noise has a negative effect on the estimation of de-ghosting parameters, but by working in sliding windows with a spatial size of about one hundred traces, and time length of the order of several hundreds of milliseconds, the effect of noise can be reduced. The data in Figure 1 represents one such window, and in a real data scenario with a constant depth streamer acquisition it would be part of a common-*p* section. The window size is a compromise between resolution – accounting for rapid changes in the ghost – and obtaining a robust estimate of parameters.

Figure 3 (top) shows the kurtosis values obtained when de-ghosting the synthetic data using the correct value for the reflection coefficient, and a range of delay-times between primary and ghost with respect to the correct value of 40ms. The correct value of 0ms is detected with high

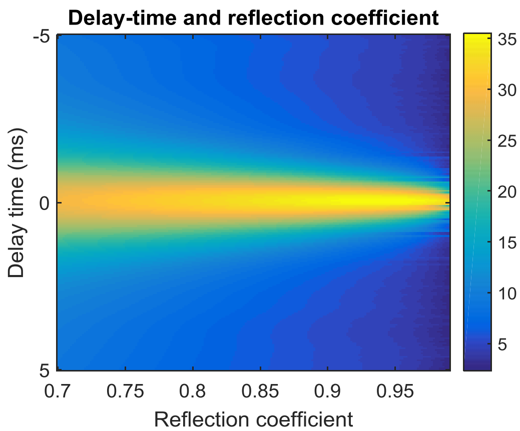

Figure 4: Kurtosis of the joint estimation of delay-time and reflection coefficient.

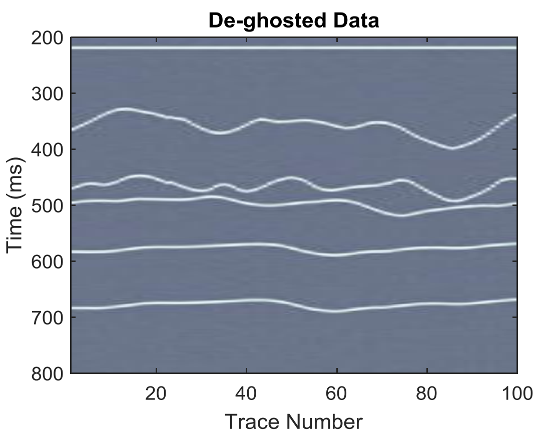

Figure 5: De-ghosting result for the data in Figure 1, after joint optimisation of delay-time and reflection coefficient based on the kurtosis values shown in Figure 4.

resolution. Figure 3 (bottom) shows the values obtained when de-ghosting the data using the correct delay-time and a variety of reflection coefficient absolute values in the range 0.7 to 1. The correct value of 0.95 is detected, although resolution is lower than for the time delay optimisation case. This is a general conclusion; the reflection coefficient is more difficult to estimate than the delay-time between primary and ghost.

To conclude this synthetic data example, Figure 5 shows the kurtosis values for the case of joint optimisation of reflection coefficient and delay-time. It can be noted that the delay-time optimisation result is broadly independent from the knowledge of the exact reflection coefficient value, while the opposite does not hold. Therefore, this optimisation problem can be solved sequentially, with the kinematic aspect of the problem (the delay-time) solved first, followed by the amplitude aspect (the reflection coefficient).

The synthetic example shown refers to a constant cable depth acquisition. For de-ghosting optimisation purposes, it is important that the recorded data is transformed to a domain where the ghost parameters are theoretically homogeneous and the domain dimensions are large, in order to have the statistical redundancy necessary for a robust estimate. The common-p domain satisfies this requirement for the constant streamer depth case, and appears particularly attractive for reflection coefficient optimization, given its higher sensitivity to noise. However, optimisation can also be carried out on τ-p transformed common-shot gathers, if shot-by shot optimization is required. The de-ghosting optimization approach discussed here is general, and can be applied also in the case of slanted streamer de-ghosting or variable depth streamer de-ghosting, after an appropriate domain transformation.

Example

We now use field data from a 2D line acquired at a constant 30m cable depth in rough sea conditions, with a significant wave height of 3m. Figure 6 shows NMO stack sections before multiple attenuation, obtained using pre-stack deterministic de-ghosting (left) and adaptive de-ghosting (right). In the case of deterministic de-ghosting, a constant reflection coefficient value of -0.9 is chosen in order to achieve a smooth average amplitude spectrum in correspondence to the first ghost notch at 25Hz, while the ghost delay-time is determined by the average cable depth during acquisition. For the adaptive de-ghosting, a single frequency-dependent reflection coefficient function was adaptively estimated for each p-section, while the delay-time was estimated in sliding and overlapping time-space windows within each common-p section. In Figure 6, a comparison of the two results, expecially in the time range 0.5 to 1s, highlights the presence of residual ghost energy in the deterministic result (left), that is not present in the adaptive result (right). The autocorrelation of the two stacked sections confirms the presence of residual ghost energy in the deterministic result with a period consistent with the ghost period at vertical incidence (40msec).

Figure 7 shows a further comparison of stack sections and autocorrelations obtained using deterministic (left) and adaptive (right) de-ghosting, followed by demultiple. We observe that demultiple effectively reduces the amount of residual ghost energy in the deterministic result. This is partly due to the fact that ringing associated with multiple events is partially removed by the demultiple, and partly due to the adaptive nature of the shallow water demultiple process used, which employs operators derived from the data itself. Nevertheless, the advantage of adaptive over deterministic de-ghosting is confirmed even after demultiple, both in terms of stack coherency and autocorrelation. In general, we expect that adaptive de-ghosting will allow for more constrained adaptive processes in the post-de-ghosting stages.

Conclusions

The parameters of the physical process determining the ghost reflection are not precisely a-priori known, and de-ghosting is highly sensitive to these parameters. In the context of parametric adaptive de-ghosting, tests on synthetic and real data suggest that the kurtosis is a useful metric in assessing de-ghosting quality and can form the basis of an objective function for an optimisation algorithm.

The adaptive procedure proposed can be sequenced in two steps. The optimisation of the ghost delay-time is robust to errors in the reflection coefficient and to noise. Therefore, it should be performed first. The reflection coefficient estimate is more sensitive to noise and requires the delay-time to be optimized in advance, and can therefore be carried out as a second step. A real data example demonstrates the applicability of the proposed method.

Acknowledgements

The data shown are provided courtesy of Dolphin's Multi-Client Department.

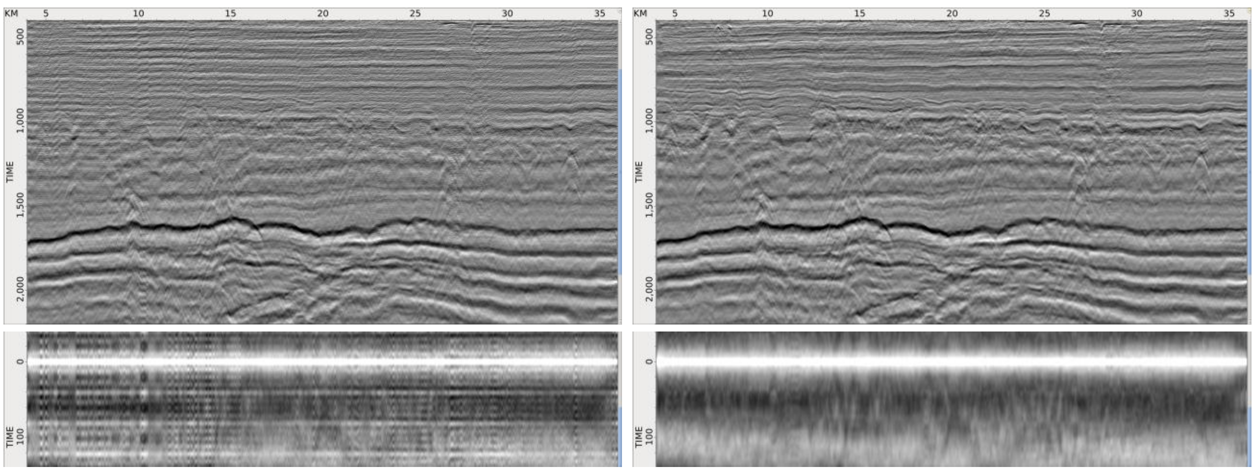

Figure 6: NMO stacks (top) and their autocorrelations (bottom) before demultiple, with deterministic de-ghosting (left) and adaptive de-ghosting (right).

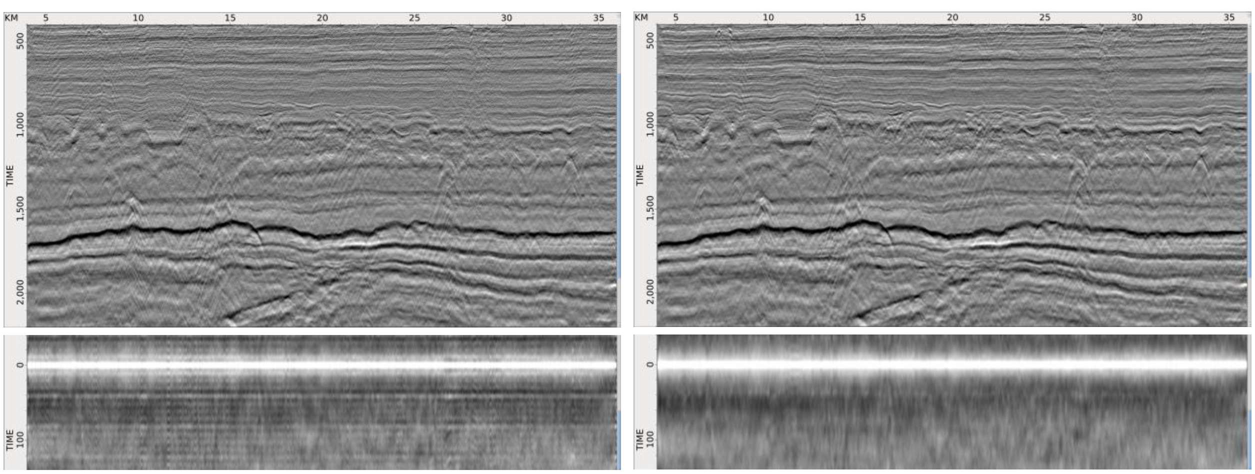

Figure 7 : NMO stacks (top) and their autocorrelations (bottom) after demultiple, with deterministic de-ghosting (left) and adaptive de-ghosting (right).

References

Grion, S., A. Azmi, J. Pollatos, N. Riddalls, and R. G. Williams, 2013, Broadband processing with calm and rough seas: observations from a North Sea survey. 83rd Annual SEG Meeting Expanded Abstracts, 226-230.

Clay, C. S. and H. Medwin, 1977, Acoustical oceanography: Principles and applications: John Wiley & Sons.

Grion, S., A. Azmi, J. Pollatos, N. Riddalls, and R. G. Williams, 2013, Broadband processing with calm and rough seas: observations from a North Sea survey. 83rd Annual SEG Meeting Expanded Abstracts, 226-230.

Grion, S., R. Telling, and J. Barnes, 2015, De-ghosting by kurtosis maximization, 77th Conference and Exhibition, EAGE, Extended Abstracts, N10306.

Masoomzadeh H., N. Woodburn, and A. Hardwick, 2013, Broadband processing of linear streamer data. 83rd Annual SEG Meeting Expanded Abstracts, 4635-4639.

Orji, O., W. Sollner, L. J., and Gelius, 2013, Sea surface reflection coefficient estimation. 83rd Annual SEG Meeting Expanded Abstracts, 51-55.

Van der Baan, M., 2008, Time-varying wavelet estimation and deconvolution by kurtosis maximization, Geophysics, **73** (2), V11-V18.

Wang, P., S. Ray, C. Peng, Y. Li, G. Poole 2013, Premigration deghosting for marine streamer data using a bootstrap approach in Tau-P domain. 83rd Annual SEG Meeting Expanded Abstracts, 4221-4225.